*Anal. Chem.* **2003,** *75,* 4859−4867

# A Tool for Studying Contact Electrification in Systems Comprising Metals and Insulating Polymers

Jason A. Wiles, Bartosz A. Grzybowski,* Adam Winkleman, and George M. Whitesides*

*Department of Chemistry and Chemical Biology, Harvard University, 12 Oxford Street, Cambridge, Massachusetts 02138*

**We describe an analytical system for in situ measurement of the charge that develops by contact electrification when a ferromagnetic sphere rolls on the surface of a polymer. This system makes it possible to survey the ability of polymeric surfaces to charge by contact electrification. Because the measurement of charge using this tool does not require physical contact of the charged sphere with the measuring electrode, it also enables the kinetics of charging to be examined. The research has focused on the contact charging of spheres having a core-and-shell geometry (a common core of ferromagnetic steel, and a variable shell of thin films of metals, or metals with surface oxides) rolling on the surface of polymeric slabs; it has generated an internally consistent set of data that include the polarity and magnitude of charging for a homologous series of polymers that differ chemically in the pendant group on a polyethylene backbone.**

This paper describes a tool for in situ measurement of the charge that develops by contact electrification on metallic spheres that roll on polymeric surfaces. We have demonstrated that this tool allows a rapid survey of the ability of polymeric surfaces to charge by indicating both the magnitude and polarity of charge as a function of time. We believe it will become a standard instrument for use in studying contact electrification because it is of simple design, easy fabrication, and convenience of use.

Contact electrification is the transfer of charge between two surfaces that are brought into contact—with or without friction—and then separated.[1−4] Contact electrification is important in widely used processes (e.g., electrophotography[5]—including photocopying and laser printing—and electrostatic separation technologies[6]); it can also be hazardous when discharge initiates vapor explosions[7] or damages electronic equipment.[8]

Although contact electrification of dielectrics is ubiquitous, it is incompletely understood.[9,10] Contact electrification is especially complicated for organic materials. Charging of organics by metals has been postulated to be due to the transfer of electrons, or ions, or both.[11,12] Independent studies of the same system of metal and organic material have given results that are inconsistent in both the magnitude and polarity of charging.[13]

The difficulties in studying contact electrification arise, in part, from the complexity of the phenomena, and in part, from lack of standard instrumentation and procedures for quantifying contact charging: the latter, in particular, leads to data that cannot be compared from one laboratory to another. Here, we describe a versatile and sensitive tool for the in situ measurement of charge that develops by contact electrification of metallic spheres that roll on surfaces of polymers. We believe this system has the simplicity required to allow screening designed to demonstrate basic relations between molecular structure and macroscopic behavior in charging. Using this tool, we quantified the contact charging of spheres having a core-and-shell geometry: a common core (ferromagnetic steel) and a variable shell (thin films of metals or metals with surface oxides) rolling on the surfaces of polymeric slabs. This paper focuses on generating an internally consistent set of data concerning charging and on clarifying discrepancies in magnitude and polarity of contact electrification that pervade the literature[14] for each metal/polymer system. In a forthcoming report, we will describe detailed studies of the kinetics of contact electrification generated by metallic spheres rolling on surfaces of polymers, including the effects of modification of the functional groups present on the surface, and of surface moisture.

Our analytical system consists of a 1-mm ferromagnetic stainless steel sphere (with or without a surface film of a different metal or metal oxide) that rolls on a flat dielectric support under the influence of an external, rotating, magnetic field (Figure 1). This system is housed in an electrically shielded, hermetic chamber. The great majority (≫99%) of the mass of the sphere is the steel core, and the contact pressure of the sphere on the surface is the same in all experiments. As the sphere rolls across the surface, it charges. This charge is measured inductively by its ability to induce charge in a thin metallic electrode placed ∼1 mm below the surface of the polymer that contacts the sphere;

* To whom correspondence should be addressed. E-mail: gwhitesides@gmwgroup.harvard.edu.

(1) Horn, R. G.; Smith, D. T.; Grabbe, A. *Nature* **1993**, *366*, 442−443.
(2) Horn, R. G.; Smith, D. T. *Science* **1992**, *256*, 362−364.
(3) Harper, W. R. *Contact and Frictional Electrification*; Laplacian Press: Morgan Hill, CA, 1998.
(4) Moore, A. D. *Electrostatics*, 2nd ed.; Laplacian Press: Morgan Hill, CA, 1997.
(5) Pai, D. M.; Springett, B. E. *Rev. Mod. Phys.* **1993**, *65*, 163−211.
(6) Kwetkus, B. A. *Part. Sci. Technol.* **1998**, *16*, 55−68.
(7) Gibson, N. *J. Electrostatics* **1997**, *40* and *41*, 21−30.
(8) Greason, W. D. *IEEE Trans. 1nd. Appl.* **1987**, *23*, 205−216.
(9) Lowell, J.; Rose-Innes, A. C. *Adv. Phys.* **1980**, *29*, 947−1023.
(10) Gibson, H. W. *Polymer* **1984**, *25*, 3−27.
(11) Diaz, A. F.; Guay, J. *IBM J. Res. Dev.* **1993**, *37*, 249−259.
(12) Guay, J.; Ayala, J. E.; Diaz, A. F.; Dao, L. H. *Chem. Mater.* **1991**, *3*, 1068−1073.
(13) Lowell, J.; Rose-Innes, A. C. *Adv. Phys.* **1980**, *29*, 947−1023.
(14) Reference 14 was removed in proof.

10.1021/ac034275j CCC: $25.00 
Published on Web 08/12/2003

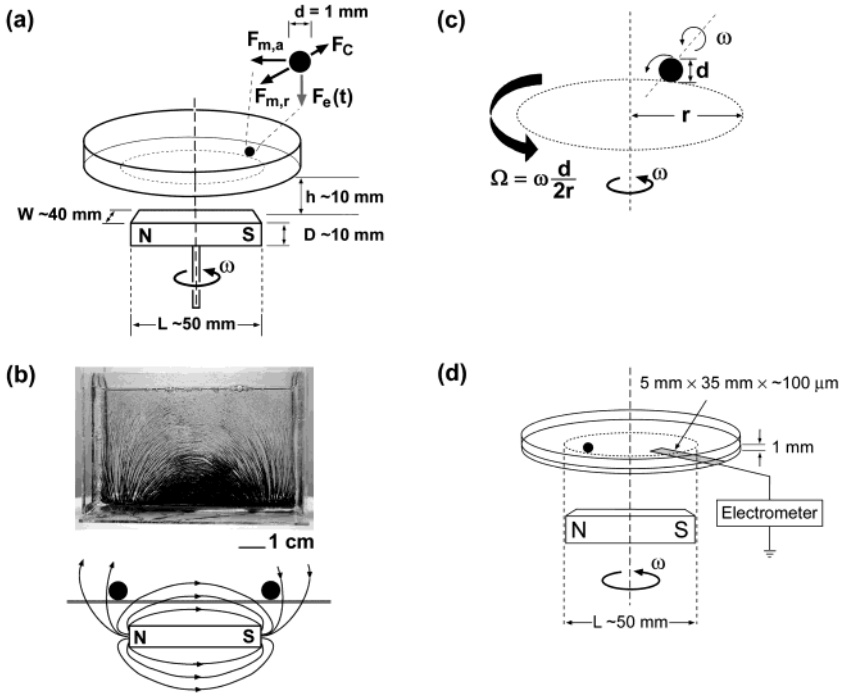


Figure 1. Experimental arrangement. (a) A ferromagnetic, stainless steel sphere 1 mm in diameter moves on a flat dielectric support under the influence of the magnetic field produced by a bar magnet rotating in the plane at angular velocity $\omega$. The forces acting on the sphere are shown in the inset ($F_{m,a}$, azimuthal magnetic force, tangential to the circular path of the sphere; $F_{m,r}$, radial magnetic force, directed toward the center of the magnetic field; $F_c$, centrifugal force, directed outward from the center of the magnetic field; $F_e(t)$, attractive electrostatic force between the surface and sphere). (b) The photograph shows the field lines produced by the rotating bar magnet that were imaged using iron filings suspended in poly(dimethylsiloxane) prepolymer (Dow Corning Sylgard 184). The sphere is confined to the annular region of the surface that experiences the highest gradient of magnetic field produced by the rotating bar magnet. Details of the magnetic force profile are described elsewhere[15,16] (c) Under the influence of the azimuthal component of the rotating magnetic field ($F_{m,a}$), the sphere rolls on the polymer surface with angular velocity $\omega$. The precession rate $\Omega$ of the sphere around the center of the magnetic field is linearly proportional to $\omega$. (d) The sphere traces a circular path on a thin polymer film (thickness ~100 $\mu$m, and supported by a 1-mm-thick PS Petri dish); this dish is electrically insulating. PS has a dielectric constant of $\epsilon = 2.6$.[39]

this electrode senses the sphere by capacitive coupling. The magnitude and polarity of the charge that accumulates on the sphere are monitored by an electrometer connected to this electrode and referenced to ground.

Although numerous devices have been developed to measure charges generated by contact electrification (e.g., spheres moving down an incline[17,18] and spheres tumbling in a rotating cylinder[19−21]), the method we describe here offers several advantages. (1) The measurement of charge is noninvasive; that is, it does not require physical contact of the sphere with the measuring electrode, and this isolation of sphere from electrode prevents loss of charge from the sphere during measurement. (2) The ability to monitor the charge as it accumulates on a sphere makes it possible to measure the *kinetics* of charging. (3) The well-defined motion of the sphere—rolling mediated by magnetic rather than gravitational forces—prevents sliding and minimizes damage to the polymer surface under examination. The controlled, magnetic actuation of the sphere ensures that the contact charging occurs as a result of rolling of the sphere on the surface, rather than by dragging, tumbling, or impact. (4) The relative humidity and atmospheric medium—factors that affect contact charging—are easily controlled and varied since the instrument is contained in a hermetic chamber.

## RESULTS AND DISCUSSION

**General Description of the Instrument.** Figure 1 illustrates the experimental arrangement. A permanent bar magnet—attached to a small motor by a rod—of approximate dimensions $L \sim 50$ mm × $W \sim 40$ mm × $D \sim 10$ mm—had magnetization $M \approx 1000$ G cm$^{-3}$ along its longest dimension[22] (Figure 1a). This magnet was located at a distance $h \sim 10$ mm below the surface of a flat dielectric support (typically a 1-mm-thick polystyrene Petri dish). With magnet stationary, a stainless steel sphere (1 mm in diameter) was placed on the surface of the polymer. This sphere was attracted toward either of the poles of the magnet (Figure 1b). When the magnet rotated, the sphere followed the path traced by the magnetic pole but at a different angular velocity. In so following, it also rotated. This motion was restricted to an annular region on the surface above the ends of the rotating magnet (Figure 1c). Under the influence of the azimuthal component of

(15) Grzybowski, B. A.; Stone, H. A.; Whitesides, G. M. *Proc. Natl. Acad. Sci. U.S.A.* **2002**, *99*, 4147−4151.
(16) Grzybowski, B. A.; Whitesides, G. M. *J. Phys. Chem. B* **2001**, *105*, 8770−8775.
(17) Gibson, H. W. *J. Am. Chem. Soc.* **1975**, *97*, 3832−3833.
(18) Gibson, H. W.; Pochan, J. M.; Bailey, F. C. *Anal. Chem.* **1979**, *51*, 483−487.
(19) Peterson, J. W. *J. Appl. Phys.* **1954**, *25*, 501−504.
(20) Peterson, J. W. *J. Appl. Phys.* **1954**, *25*, 907−915.
(21) Wagner, P. E. *J. Appl. Phys.* **1956**, *27*, 1300−1310.
(22) Grzybowski, B. A.; Stone, H. A.; Whitesides, G. M. Nature **2000**, *405*, 1033−1036.

the rotating magnetic field, the sphere traced a circular path on the surface. For each revolution of the external magnet, the sphere performed one rotation around approximately the axis joining its center and the center of the magnet.[23] This relationship demonstrated that the sphere rolled (rather than slid) on the surface of the dielectric. The rate of precession of the sphere ($\Omega \approx 20$ rpm) was approximately a linear function (see Figure 1c) of the rate of rotation of the external magnet (and hence the external magnetic field: $\omega \approx 1000$ rpm) with the constant of proportionality equal to the ratio of the circumference of the sphere (in our experiments, 3.14 mm) to the circumference of the circular path the sphere traced on the surface (~157 mm). As the metallic sphere rolled across the surface of the film, the sphere and the surface developed charges of equal magnitude and opposite polarity via contact electrification.[24] The magnitudes of these charge increased with time.

**Measurement of Contact Electrification.** The charge (both magnitude and polarity) on the sphere was measured as follows. A film of the polymer to be examined was cast from solution onto a 1-mm-thick support (Petri dish) of polystyrene (PS) or Pyrex (polymers soluble in aqueous solution were cast on PS and polymers soluble in organic solvents were cast on Pyrex) and was dried thoroughly in an oven; free-standing films were attached to supports of PS by epoxy resin. An electrode of aluminum foil[25] (5 mm × 35 mm × 100 $\mu$m) was attached to the bottom of the support using adhesive, electrically insulating tape, and was connected to an electrometer (Figure 1d). The entire setup, excluding electrometer, was housed in a hermetic chamber surrounded by an electrically shielding Faraday cage. A sphere was gently placed on the film when the external magnet was stationary, and any adventitious charge on the sphere and film was neutralized thoroughly by applying negative and positive ions from a corona discharge using a piezoelectric antistatic gun (Zerostat).[26] All data were collected at 21−24% relative humidity (RH) and 23 °C, unless noted otherwise; these values were monitored using a digital hygrometer/thermometer. Every time the sphere of charge $Q_S$ rolled on the part of the surface above the metallic electrode, it induced a charge $Q_{Ind}$ on this electrode; the polarity of $Q_{Ind}$ was opposite to that of $Q_S$. The charge measured by the electrometer $Q_M$ as a potential difference of its internal capacitor[27] was the opposite of the charge induced in the electrode, $Q_M = -Q_{Ind}$. Thus, the measured charge had the same polarity as the charge on the sphere (the relationship between the *magnitudes* of the two charges will be discussed in the next section). The magnitude of $Q_M$ increased monotonically with time up to a saturation value. The polarity of the induced charge, its maximal value, and the rate of charging were characteristic for each pair of materials (film and sphere). Figure 2 is a typical plot of the time-dependent charge on a stainless steel sphere rolling on a film of polyacrylamide ($PCONH_2$). The *upward*, periodically spaced signals in the plot (and in other plots in this paper) correspond to a *positively* charged sphere passing over the electrode. It is not crucial to have a stable (drift-free) electrometer to measure the charge on the sphere because the procedure involves differential measurement. The precision of the charge measurement is typically 5−10%, as judged by comparing the height of the signals over a short period of time in a typical plot of $Q_M(t)$ (e.g., see Figure 2).

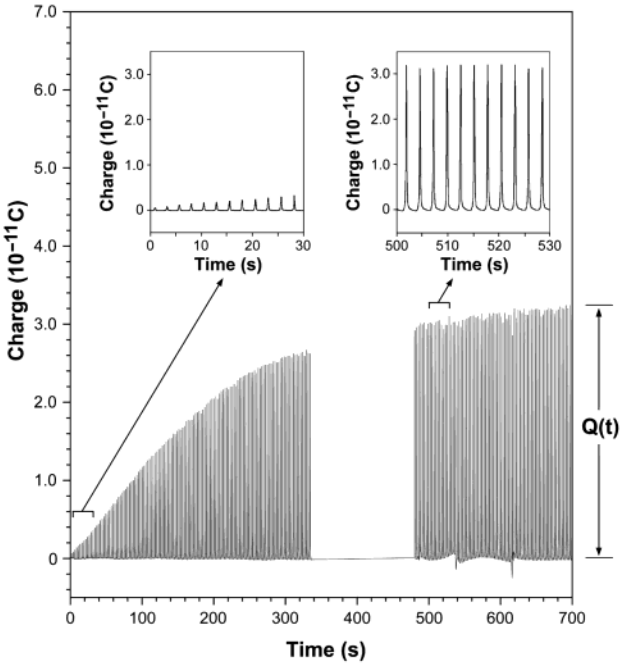


Figure 2. Time-dependent charge on a stainless steel sphere rolling on a film of $PCONH_2$. The inset on the left shows the initial charging profile; the inset on the right shows the selected region when near-maximum charge accumulated on the sphere. The upward signals in each plot, which are periodically spaced (time of precession of the sphere on the surface), designate instances when the positively charged sphere is near the metallic electrode, registering induced charge. The gap of ~150 s during the acquisition of data (330 s ≤ $t$ ≤ 480 s) is a consequence of the limited storage capacity of the digital electrometer (~330 s of data). The collection of data resumed ($t$ > 480 s) after the previous data were transferred (requiring ~150 s) to a PC for processing.

**Calibration of the Instrument. (i) Experimental Dependence of $Q_M$ on the Width of the Electrode $d$.** Because an

(23) Grzybowski, B. A.; Wiles, J. A.; Whitesides, G. M. *Phys. Rev. Lett.* In press.

(24) We confirmed this relationship by measuring the charges that developed on a polymeric sphere (available from Small Parts and made of Teflon, poly(methyl methacrylate), or polypropylene) that rolled on the surface of a horizontally vibrated, metallic surface (i.e., a PS Petri dish coated with a thermally evaporated layer of gold, silver, or chromium) and that on the metallic surface itself. After the sphere rolled on the surface and charged, the magnitude and polarity of the charge acquired on the insulating sphere was determined by removing it from the metallic surface and placing it in a Faraday cup that was connected to an electrometer; the magnitude and polarity of the acquired charge on the metal was determined by connecting this conducting surface to the electrometer after tribocharging. The charges on the sphere and surface were of opposite polarity and of approximately equal magnitude.

(25) Electrodes of copper and gold were used also. The magnitudes of the charge measured using electrodes of aluminum, copper, and gold were indistinguishable.

(26) A corona discharge occurs at the front of the antistatic instrument between two electrodes. Slowly squeezing the trigger (lasting 1−2 s) produces a stream of positive ions and slowly releasing the trigger produces a stream of negative ions. The positive ions generated by corona discharge in air are composed of $H^+(H_2O)_n$ ($n$ = 1, 2, 3, ...) and the negative ions of $CO_3(H_2O)_n$, $O_2(H_2O)_n$, $NO_3(H_2O)_n$, $NO_2(H_2O)_n$, $O^-(H_2O)_n$, and $O_3(H_2O)_n$ (Sakata, S., Okada, T. *J. Aerosol Sci.* **1994**, *25*, 879−893). Any adventitious charge was neutralized by squeezing and releasing the trigger of the gun (~10 times) that was positioned ~5 cm above the sphere and film.

(27) The charge was detected as a potential difference across an accurately known capacitor in the electrometer. The voltage was scaled according to the equation $V = Q/C$ (where $V$ is potential difference, $Q$ is charge, and $C$ is capacitance) and was displayed as charge on the digital readout of the electrometer.

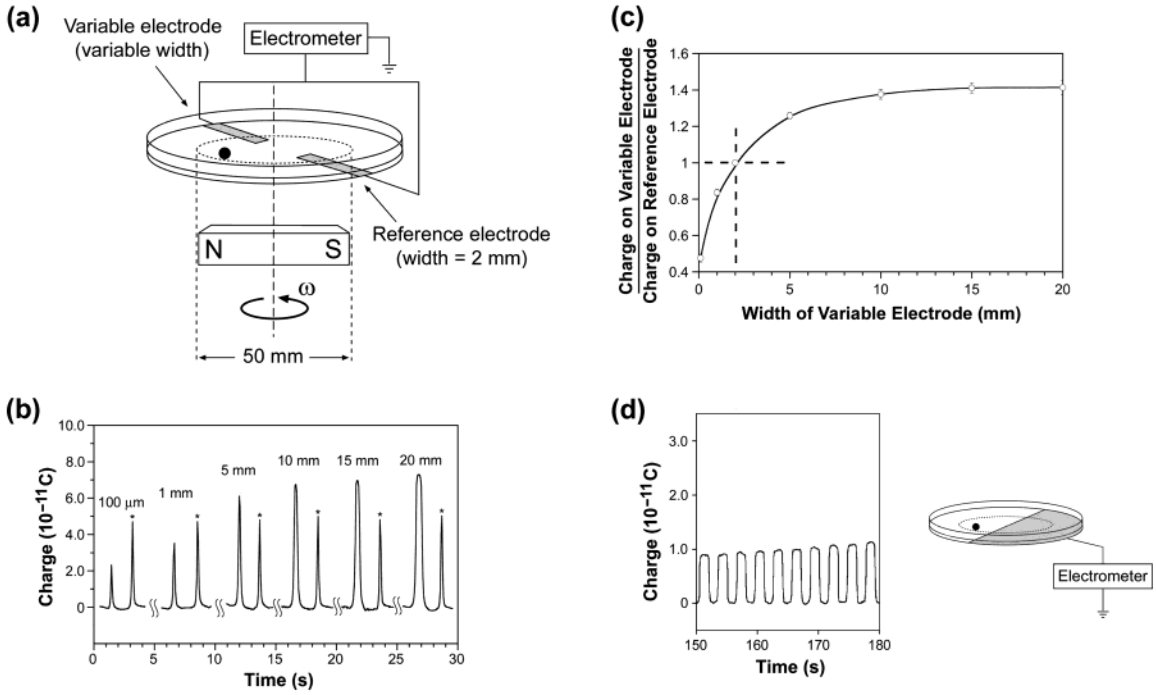


Figure 3. (a) Experimental arrangement for determining the relationship between the width of the metallic electrode and the magnitude of the charge induced in the electrode by the stainless steel sphere. Two metallic electrodes (one variable in width, one fixed) are connected to the same electrometer; both electrodes measure charge on the sphere as it rolls over the surface of PS. The measurement by the working electrode is calibrated with respect to the 2-mm-wide reference electrode. (b) Data from six independent experiments where the width of the variable electrode was changed (100 $\mu$m to 20 mm). Each experiment generates two values of charge, one for each electrode. Experiments are separated by hatch marks. The signals on the left are those measured by the variable electrodes, and the signals on the right (indicated by asterisks) are those measured by the 2-mm-wide reference electrode. (c) The charge a stainless steel sphere induces in a metallic electrode as a function of the width of the electrode. The data in this plot are given as the ratio of the magnitude of the charge measured by the variable electrode to that of the reference electrode. (d) The experimental setup for measuring the charge induced by a stainless steel sphere in an electrode covering half of a surface of PS. A plot of the time-dependent, square-wave signal of charge is given on the left.

electrode of a large surface area detects more electric field lines emanating from a charged sphere rolling above it than an electrode of a small surface area, we expected that the magnitude of the charge $Q_M$ measured by the electrometer should increase monotonically with the width of the electrode $d$. We studied the dependence of $Q_M$ on $d$ using an experimental setup shown in Figure 3a. This setup is similar to that in Figure 1 with the exception that there are now two metallic electrodes below the surface of the polymer. Since both electrodes are connected to the same electrometer, the measurement is self-calibrating. We kept one of the aluminum electrodes at a constant width (2 mm); this electrode served as a reference electrode. We used a range of widths (from 100 $\mu$m to 20 mm) for the second, variable electrode. Figure 3b shows results from six experiments in which the width of the variable electrode was changed. Two signals (all recorded at the same times from the beginning of rolling) are shown for each experiment: signals on the left are those measured by the variable electrodes, and signals on the right are those measured by the reference electrode (marked by asterisks). From these experiments we conclude the following: (i) the measured charges increase with increasing $d$, (ii) the widths of the signals also increase with $d$ (cf. Figure 3d),[28] (iii) the maximal detected charge corresponds to the position of the sphere above the center of the electrode, and (iv) increasing the width of the electrode beyond ~10 mm does not increase the magnitude of $Q_M$.

**(ii) Functional Relationship between $Q_M$ and $d$.** Figure 3c illustrates how the ratio of the charge measured by the variable electrode of width $d$ to the charge measured by the reference electrode ($Q_M(d)/Q_M(d = 2$ mm)) depends on the width of the variable electrode. The functional form of this dependence is found using the method of images.[29] Let the dimensions of the electrode be $d = 2W$ by $2L$, where $W \ll L$, and the frame of reference be chosen such that the center of the charged sphere (of charge $Q_S$) is above the center of the electrode (Figure 4a); the distance between the two centers is denoted $H$. An image sphere of charge $-Q_S$ is placed symmetrically on the opposite side of the electrode. The magnitude of the electric field at the location $(x, y)$ on the surface of the electrode is obtained by the superposition of the fields produced by the two spheres as in eq 1. The charge $Q_{Ind}$ induced in the variable electrode is given by the surface integral of $E$ (eq 2). Substituting the dimensions of the electrode, and using

$$E = (Q_S H/4\pi\epsilon)(x^2 + y^2 + H^2)^{-3/2} \quad (1)$$

$$Q_{Ind} = \int_{surface}\int \epsilon E \, dx \, dy \quad (2)$$

(28) This hypothesis was confirmed after observing that the width of the signals increased to half of the period of precession of the sphere when using a metallic electrode that covered half of the annular region of the PS surface over which the sphere rolled (see Figure 3d).

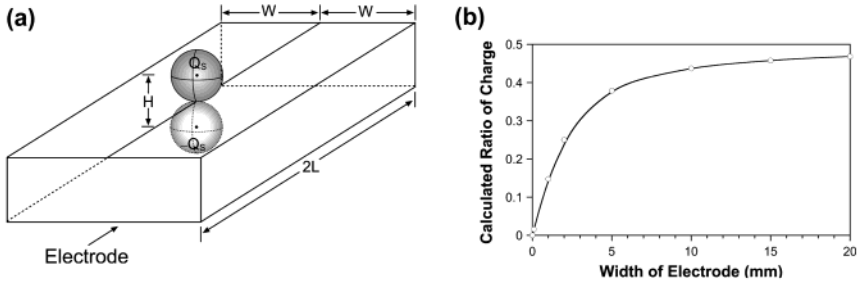


Figure 4. (a) Schematic illustration of the geometric arrangement used to derive eq 4. Electric field in the plane of the electrode is calculated from the superposition of fields produced by the metallic sphere of charge $Q_S$ and a symmetrically placed image sphere of charge $-Q_S$. Charge induced in the electrode is calculated by integrating the electric field over the area of the electrode. (b) The plot of the ratio of charge $Q_M$ measured by our device to the actual charge $Q_S$ of the rolling sphere as a function of the width $d = 2W$ of the electrode. Calculation was done with $H = 1$ mm.

symmetry, we obtain eq 3. Integrating with respect to $x$, and noting

$$Q_{Ind} = Q_S H/\pi \int_0^W \int_0^L (x^2 + y^2 + H^2)^{-3/2}\, dx\, dy \qquad (3)$$

that $L^2 \gg W^2 + H^2$ and that $Q_M = -Q_{Ind}$, this integral simplifies to eq 4. The plot of $Q_M/Q_S$ as a function of the width of the

$$Q_M = \frac{Q_S H}{\pi} \int_0^W (y^2 + H^2)^{-1} dy = \frac{Q_S}{\pi} \arctan\frac{W}{H} \qquad (4)$$

electrode $2W$ and with $H = 1$ mm is given in Figure 4b and is qualitatively similar to the experimental dependence in Figure 3c.

**(iii) Relation between $Q_M$ and $Q_S$.** For a given width of the electrode, eq 4 relates the charge measured by the electrometer to the actual charge on the rolling sphere. We verified this relationship experimentally. We measured $Q_S$ using a Faraday cup and compared it to $Q_M$ measured by the electrometer connected to a 5-mm-wide electrode (at this width, the electrode gave very sharp peaks and high signal-to-noise ratios). We first rolled a metallic sphere on a PS support and recorded the charge it developed as a function of time. At a specified time, we transferred the sphere to a Faraday cup connected to an electrometer. We repeated this experiment several (~10) times, each time using a new sphere and changing the times of rolling. We found that the ratio of charges recorded by the electrometer at the time of transfer to the charge measured by the Faraday cup (that is, $Q_M/Q_S$) was ~0.35 (±6%), in excellent agreement with the value of 0.38 predicted by eq 4.

**(iv) Surface Charges and Electroneutrality.** The total charge developed on the surface of the polymer $Q_{Surf}$ is equal in magnitude, and has polarity opposite to, the charge on the rolling sphere $Q_S$. This equality was confirmed by two types of measurements: (a) When both the spheres and the Petri dish in which they rolled were placed in a Faraday cup, the electrometer showed no net charge on the system; i.e., $Q_{Surf} + Q_S = 0$; (b) when the spheres and the dish were transferred to the Faraday cup separately, the electrometer indicated that both $Q_{Surf}$ and $Q_S$ were nonzero and that $Q_{Surf} = -Q_S$.

**Quantitative Study of Contact Electrification.** We first focused on clarifying the polarities and magnitudes of contact electrification of metallic spheres that roll on polymeric surfaces. We examined 16 different polymeric films and 5 metals and metal oxides (Table 1). Data were collected at 21−24% RH and 23 °C using the instrument depicted in Figure 1 using a 5-mm-wide electrode; the width of this electrode ensures generation of data having a large signal-to-noise ratio (see Figure 3). Table 1 lists the *maximum* (saturation) values of charge generated on the spheres that roll on each of the dielectric films; each entry is the average value of five measurements that used fresh films and spheres for each measurement to avoid contamination of samples. The polymer films that we examined are listed in the left-hand columns, and the materials on the surface of the stainless steel spheres are listed in the top row of Table 1. "Silver" designates a stainless steel sphere that had been coated with a 300-nm layer of silver; "silver oxide" designates a stainless steel sphere that had been coated with a 300-nm layer of silver and subsequently oxidized in a 30% solution of hydrogen peroxide. Plus and minus symbols preceding numeric values in Table 1 designate the positive and negative polarity of the charges measured on the metallic spheres, respectively. In cases where the charge that accumulated on a sphere was large (typically $\geq 8 \times 10^{-11}$ C or $5 \times 10^8$ electrons, but this value is lower for soft polymer supports), the sphere adhered to the surface of the film because the electrostatic forces between the sphere and the film were greater than the motive magnetic force.[30] The parentheses denote instances when a sphere adhered to a film; the values are the maximum magnitude of charges accumulated on a sphere before the sphere adhered to the film (the absence of a value indicates that the sphere would not roll on the surface). The ordering of the polymers in Table 1 forms an approximate triboelectric series, with the most negatively charging polymers following the most positively charging polymers from top to bottom.

We determined the sign and magnitude of charging for a related series of poly(olefins) ($-CH_2CHX-$)—differing only by the pendant group on the polyethylene backbone—that include polyacrylamide ($PCONH_2$), poly(acrylic acid) (PAA), poly(allylamine) ($PCH_2NH_2$), polyethylene (PE), poly(hexyl methacrylate) (PHMA), poly(methyl acrylate) (PMA), poly(methyl methacrylate) (PMMA), polystyrene (PS), poly(vinyl acetate) (PVAc), poly(vinyl alcohol)

(29) Crowley, J. M. *Fundamentals of Applied Electrostatics*; Laplacian Press: Morgan Hill, CA, 1999.

(30) Neutralizing the system by applying negative and positive ions from a corona discharge after the sphere adhered to the surface allowed the sphere to continue rolling under the influence of the rotating magnetic field.

Table 1. Comparison of the Ability of Materials To Charge by Contact Electrification[a]

| | | | gold | "gold oxide" | "silver" | "silve oxide" | steel | |
|---|---|---|---|---|---|---|---|---|
| polystyrene[b] | PS[b] | Petri dish | (+9.9) | (+14.0) | (+11.0) | (+14.8) | (+15.0) | Ⓟ-Ph |
| poly(tetrafluoroethylene) | PTFE | film | (+6.7) | +7.4 | (+7.3) | (+7.5) | (+6.3) | $[CF_2CF_2]_n$ |
| poly(acrylic acid)[c] | PAA[c] | cast (aq) | +4.0[d] | +3.0[d] | +3.8[d] | +3.3 | +3.8[d] | Ⓟ-$CO_2H$ |
| borosilicate glass | Pyrex | Petri dish | +4.0 | +1.4 | +2.1 | +3.0 | +5.0 | Si-OH/B-OH |
| poly(vinyl chloride) | PVC | film | +3.5 | +1.5 | +1.5 | +2.1 | +1.5 | Ⓟ-C1 |
| polyacrylamide | $PCONH_2$ | cast (aq) | +3.3 | +2.6 | +3.5 | +1.9 | +4.1 | Ⓟ-$CONH_2$ |
| poly(ethylene terephthalate) | Mylar | film | +2.4 | +4.3 | +1.8 | +3.2 | +2.5 | see below |
| poly(allylamine) | $PCH_2NH_2$[c,e] | cast (aq) | 0.0 | 0.0 | 0.0 | 0.0 | 0.0 | Ⓟ-$CH_2NH_2$ |
| poly(bisphenol A carbonate) | Lexan | film | −0.4 | −0.4 | −0.4 | −1.2 | −0.3 | see below |
| polyethylene | PE | cast (tol) | −0.7 | −1.0 | −0.8 | −0.2 | −0.5 | Ⓟ-H |
| poly(hexamethylene-adipamide) | Nylon-6,6 | film | −3.5 | (−10.6) | −3.8 | (−9.2) | −2.5 | see below |
| poly(hexyl methacrylate)[c] | PHMA[c] | cast (tol) | (−4.2) | (−4.3) | (−4.6) | () | () | $CH_3$-Ⓟ-$CO_2C_6H_{13}$ |
| poiy(methyl methacrylate) | PMMA | cast (tol) | −8.2 | (−10.1) | −8.6 | −8.9 | −9.3 | $CH_3$-Ⓟ-$CO_2CH_3$ |
| poly(methylacrylate) | PMA | cast (tol) | (−8.8) | (−7.5) | −7.4 | (−7.7) | (−9.0) | Ⓟ-$CO_2CH_3$ |
| poly(vinyl alcohol) | PVA | cast (aq) | (−10.5) | (−11.6) | (−9.5) | (−12.0) | (−10.8) | Ⓟ-OH |
| poly(vinyl acetate) | PVAc | cast ($CH_2Cl_2$) | (−12.0) | (−9.5) | (−9.4) | (−9.7) | (−11.4) | Ⓟ-$OCOCH_3$ |

[a] The values listed are maximum charge ($10^{-11}$ C) measured on a given kind of sphere (column heading) after rolling on a particular substrate (two left columns). Each value is the average of five measurements (standard deviation ∼10%) that were taken at 21−24% RH and $T$ = 23 °C; values within parentheses represent the maximum charge on the sphere prior to it adherence to the film. The symbol "Ⓟ" represents the polyethylene backbone of the polymer. [b] PS Petri dishes typically have ∼1 atom % oxygen on their surface. We infer that dishes used in this s;tudy had similar contents of oxygen by comparing contact angles of water on their surfaces with those reported previously (Dupont-Gillain, Ch. C.; Adriaensen, Y.; Derclaye, S.; Rouxhet, P. G. *Langmuir* **2000**, *16*, 8194−8200). [c] Film was dried in an oven (60 °C, ∼1 mmHg, ∼12 h) followed by a vacuum oven (60 °C, ∼1 mmHg, ∼12 h). [d] Periodic charging where spheres reach the indicated levels of charge, adhere to the film, and continue to roll after the charge dissipates. [e] For all spheres, the charge detected was $<0.05 \times 10^{-11}$ C.

(PVA), and poly(vinyl chloride) (PVC).[31] (We also included the commonly studied polymers Lexan, Mylar, Nylon-6,6, poly(tetrafluoroethylene) (PTFE), and Pyrex for completeness.) The saturated carbon backbone in this series of polymers is a common feature and is inert to charging (that is, PE appears not to charge). We assume that the pendant groups dominate the charging of these polymers.

Table 1 and Figure 5 show, with few exceptions, that the charging of the sphere is determined by the polymer and is independent of the metal/metal oxide on the surface of the sphere. Different metals charge to the same extent on the same polymers; the same metal charges to different extents on different polymers. To confirm that the surface groups of the polymer are responsible for the observed contact electrification, we transformed the surface of PAA films into PMA by reaction with diazomethane for 30 min (eq 5). The polarity of the charge resulting from contact electrification of all metal and metal oxides rolling on a surface of methylated PAA was the same as that observed for pure PMA (Table 2). The magnitude of the charge was only 30% that observed for authentic PMA; the difference may be due to the effects of the bulk PAA below the thin modified surface, the rearrangement of the surface groups, or the incomplete reaction of the surface groups. We favor rearrangement of the newly formed ester surface groups—rearrangements previously observed in poly(methacrylate)s[32,33]—because the $T_g$ of the newly formed PMA (10 °C compared with 106 °C for PAA) on the surface is below the temperature of the experiment; at this temperature, the polymer chains are mobile, and the surface groups should interchange readily with subsurface groups. An incomplete reaction on the surface is unlikely because we did not observe any further increase in the magnitude of charging upon further reaction (an additional 30 min) with diazomethane and because reactions of diazomethane with carboxylic acids proceed rapidly and in high yield.

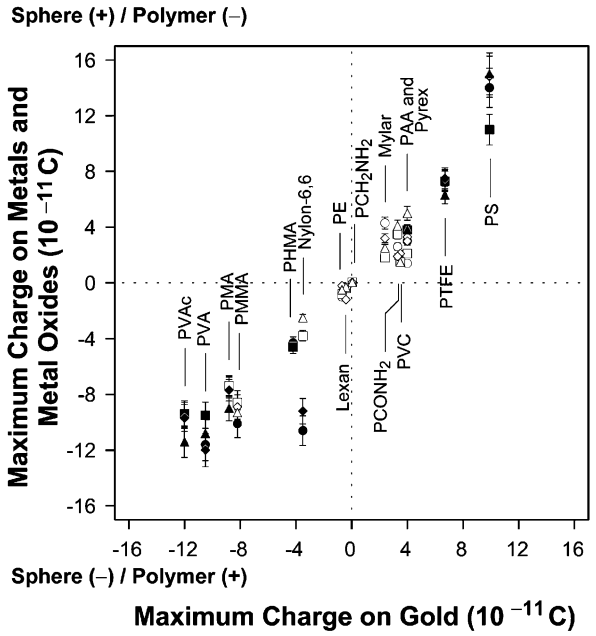


Figure 5. Maximum charges measured on "gold oxide" (○/●), "silver" (□/■), "silver oxide" (◇/◆), and steel (△/▲) as a function of the maximum charge measured on gold for a given dielectric surface. Open markers represent saturation data, and closed markers represent the maximum magnitude of charges accumulated on a sphere before the sphere adhered to the film.

(31) Homologous series of polymers were previously examined to study the mechanism of contact electrification, but in these studies, the series were small and the polymers were usually derivatives of PS (Gibson, H. W. *Polymer* **1984**, *25*, 3−27).

(32) Chen, Q.; Zhang, D.; Somorjai, G.; Bertozzi, C. R. *J. Am. Chem. Soc.* **1999**, *121*, 446−447.

(33) Wang, J.; Woodcock, S. E.; Buck, S. M.; Chen, C.; Chen, Z. *J. Am. Chem. Soc.* **2001**, *123*, 9470−9471.

Table 2. Confirmation That Surface Groups Are Responsible for the Observed Contact Charging. Reaction of PAA and Diazomethane To Generate PMA[a]

| | | gold | "gold oxide" | "silver" | "silver oxide" | steel | |
|---|---|---|---|---|---|---|---|
| poly(acrylic acid)[b] | PAA[b] | +4.0[c] | +3.0[c] | +3.8[c] | +3.3 | +3.8[c] | Ⓟ-$CO_2H$ |
| poly(acrylic acid) + diazomethane[b] | PAA[b] + $CH_2N_2$ | −2.1 | −2.5 | −2.6 | −1.0 | −2.7 | Ⓟ-$CO_2H/CH_3$ |
| poly(methylacrylate) | PMA | (−8.8) | (−7.5) | −7.4 | (−7.7) | (−9.0) | Ⓟ-$CO_2CH_3$ |

[a] The values listed are maximum charge ($10^{-11}$ C) measured on a given sphere (column heading) after rolling on a particular substrate (two left columns). Each value is the average of five measurements (standard deviation ~10%) that were taken at 21−24% RH and $T = 23$ °C; values within parentheses represent the maximum charge on the sphere prior to it adhering to the film. The symbol "Ⓟ" represents the polyethylene backbone of the polymer. [b] Film was dried in an oven (60 °C, ~12 h) followed by a vacuum oven (60 °C, ~1 mmHg, ~12 h). [c] Periodic charging where spheres reach the indicated levels of charge, adhere to the film, and continue to roll after the charge dissipates.

Table 3. Effects of Water and Temperature on the Ability of Materials To Charge by Contact Electrification[a]

| | | | gold | "gold oxide" | "silver" | "silve oxide" | steel | |
|---|---|---|---|---|---|---|---|---|
| poly(acrylic acid)[b] | PAA[b] | 23 °C | +0.3 | −0.2 | +0.3 | −0.2 | +0.3 | Ⓟ-$CO_2H$ |
| poly(acrylic acid)[c] | PAA[c] | 23 °C | +4.0[d] | +3.0[d] | +3.8[d] | +3.3 | +3.8[d] | Ⓟ-$CO_2H$ |
| poly(acrylic acid)[b] | PAA[b] | 6 °C | +4 3[d] | +2.6 | +3.5[d] | +1.7 | +3.5[d] | Ⓟ-$CO_2H$ |
| poly(allylamine)[c] | $PCH_2NH_2$[e] | 23 °C | 0.0 | 0.0 | 0.0 | 0.0 | 0.0 | Ⓟ−$CH_2NH_2$ |
| poly(allylamine) | $PCH_2NH_2$ | 6 °C | −3.0[d] | −3.6[d] | −3.6[d] | −3.9[d] | −2.3[d] | Ⓟ−$CH_2NH_2$ |

[a] The values listed are maximum charge ($10^{-11}$ C) measured on a given sphere (column heading) after rolling on a particular substrate (two left columns). Each value is the average of five measurements (standard deviation ~10%) that were taken at 21−24% RH and $T = 23$ °C, unless noted otherwise; values within parentheses represent the maximum charge on the sphere prior to it adhering to the film. The symbol "Ⓟ" represents the polyethylene backbone of the polymer. [b] Film was dried in an oven (60 °C, ~12 h). [c] Film was dried in an oven (60 °C, ~12 h) followed by a vacuum oven (60 °C, ~1 mmHg, ~12 h). [d] Periodic charging where spheres reach the indicated levels of charge, adhere to the film, and continue to roll after the charge dissipates. [e] For all spheres, the detected charge was $< 0.05 \times 10^{-11}$ C.

**Influence of Water Content in the Polymer and Temperature on Contact Electrification.** We prepared films of PAA, $PCONH_2$, $PCH_2NH_2$, and PVA from aqueous solution, and we observed that the contact electrification of two of these polymers (PAA, $PCH_2NH_2$) was strongly influenced by water content (Table 3). In particular, an aqueous solution of PAA, cast on a support and dried in an oven at 60 °C overnight, showed little charge separation with all of the metals ($+0.3 \times 10^{-11}$ C) and metal oxides ($-0.3 \times 10^{-11}$ C). More importantly, the widths of the signals in the plots of time-dependent charge for PAA (Figure 6a) are broader than those observed for other surfaces (cf. $PCONH_2$, Figure 2). We reasoned that the increase in peak width might be caused by dissipation of the charge on the sphere through the polymer (or across its surface) via a weakly conductive network of water; i.e., the metallic electrode detects the charge on the sphere rolling on PAA at distances greater than that required for less conductive surfaces. In support of this hypothesis, increasing the width of the electrode causes an increase in the width of the signal (Figure 3), and lowering the temperature of the film of PAA to 6 °C causes the signals to sharpen to the typical line widths (Figure 6b). Further support for leakage of charge via water is that, upon removal of water from PAA (12 h in a vacuum oven, 60 °C, ~1 mmHg), the width and magnitude of the signals recorded at 23 °C are similar to those recorded for the film containing water at 6 °C (Figure 6c).

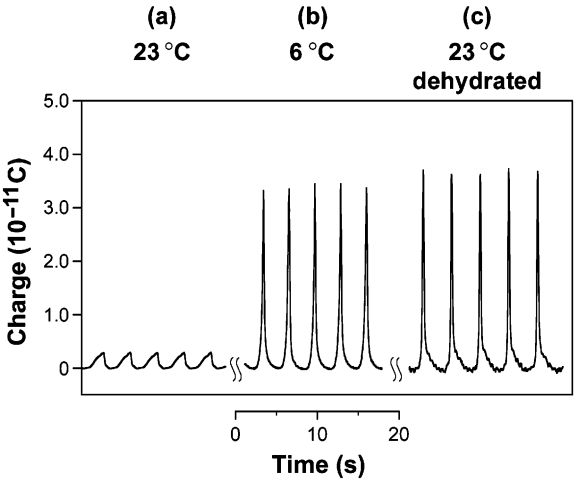


Figure 6. Time-dependent charge on a stainless steel sphere rolling on films of PAA that were cast from aqueous solution. Data from three independent experiments are shown; five signals are shown for each experiment and are separated from those of other experiments by hatch marks. (a) The film was dried in an oven at 60 °C for ~12 h; data were collected at 23 °C. (b) The film was dried in an oven at 60 °C for ~12 h; data were collected at 6 °C. (c) The film was dried in an oven at 60 °C for ~12 h followed by a vacuum oven (~1 mmHg) at 60 °C for ~12 h; data were collected at 23 °C. All data are at steady state (after >3 min of rolling).

We also observed that spheres charge to the values indicated in Table 3 and then adhere to the surfaces of PAA and $PCH_2NH_2$ though electrostatic interactions. Once the charge on the sphere dissipates through the conductive surface of the moist polymer, the sphere is electrically neutral and again rolls, acquiring charge to the previously observed value until it adheres to the surface of the polymer. The cycle then continues; $PCH_2NH_2$ shows similar behavior. Although other workers have proposed leakage of charge on surfaces to account for the affects of RH on contact electrification, they were not able to observe this phenomenon directly.[34] Investigating contact electrification of metallic spheres

on polymers containing water demonstrates the power of our technique to observe directly leakage of charge on a conductive surface.

**Exclusive Ion- or Electron-Transfer Mechanisms Cannot Explain Contact Electrification.** In work prior to ours, small sets of data have been interpreted as suggesting a single mechanism—either electron transfer or ion (proton) transfer—for contact charging. For example, Akande and Lowell[35] observed that the charge on the polymers in the series PMMA, PS, PVA, PVAc, and PVC does not depend on the work function of the contacting metal; this observation is inconsistent with an electron-transfer mechanism. Gibson and Bailey[36] proposed that the charging process involved electron transfer based on the observation that the logarithm of the magnitude of contact charging (essentially initial rates of charging because their times of contact were constant and on the order of $\sim 10^{-5}$ s) of a small homologous series of polymers (PS, PVC, poly(acrylonitrile) (PAN), PVAc) with nickel spheres correlated linearly by inductive substituent constants ($\sigma_{I,X}$, where X is the substituent on Ⓟ-X). In this series, PAA and PVA were also examined but deviated significantly. They argued in support of their interpretation that both the ionization potential[37] and the electron affinity of the polymer increase in proportion to $\sigma_{I,X}$.[38] Proton affinities also, of course, correlate with $\sigma$ constants and were in fact used to derive them, so a correlation of this sort does not distinguish between electron and ion transfer. Although the steady-state data presented in Table 1 prevent a quantitative correlation of the magnitudes of contact electrification with chemical structure of the polymers or metals (the magnitude of the charge on spheres that adhere to a film is equal to or greater than that listed in Table 1), the observed data correlate only poorly with $\sigma_{I,X}$ (Figure 7). Table 1 and Figure 5 show that the charges on the polymers are increasingly more negative in the series PS > PAA > PVC; this ordering is the reverse of that observed by Gibson and Bailey. Also, in contrast to data reported by Gibson and Bailey, but in accord with data reported by others,[39,40] we have found that PVA, PVAc, and PMMA charge with positive polarity when contacted by all of the metals and metal oxides examined. While we did not examine the contact electrification of nickel-coated spheres, we note that the work function of nickel ($\sim$5.2 eV) is within the range of work functions of metals that we examined (gold is $\sim$5.4 eV and silver is $\sim$4.7 eV).[41] The differences between our results and those of Gibson and Bailey may be due to the method of charge measurement. We have observed that if a surface and sphere are discharged incompletely prior to an experiment, erroneous results occur; i.e., adventitious charge of the incorrect polarity is initially on the sphere, which reverts through contact charging to the correct magnitude and polarity. This initial, incorrect charging behavior is detectable using our technique because we monitor charging with time; it is impossible to detect using the technique of Gibson because this technique only measures (using a Faraday cup) the *final* charge accumulated on a sphere after it moves down an inclined plane for short contact times ($\sim 10^{-5}$ s).

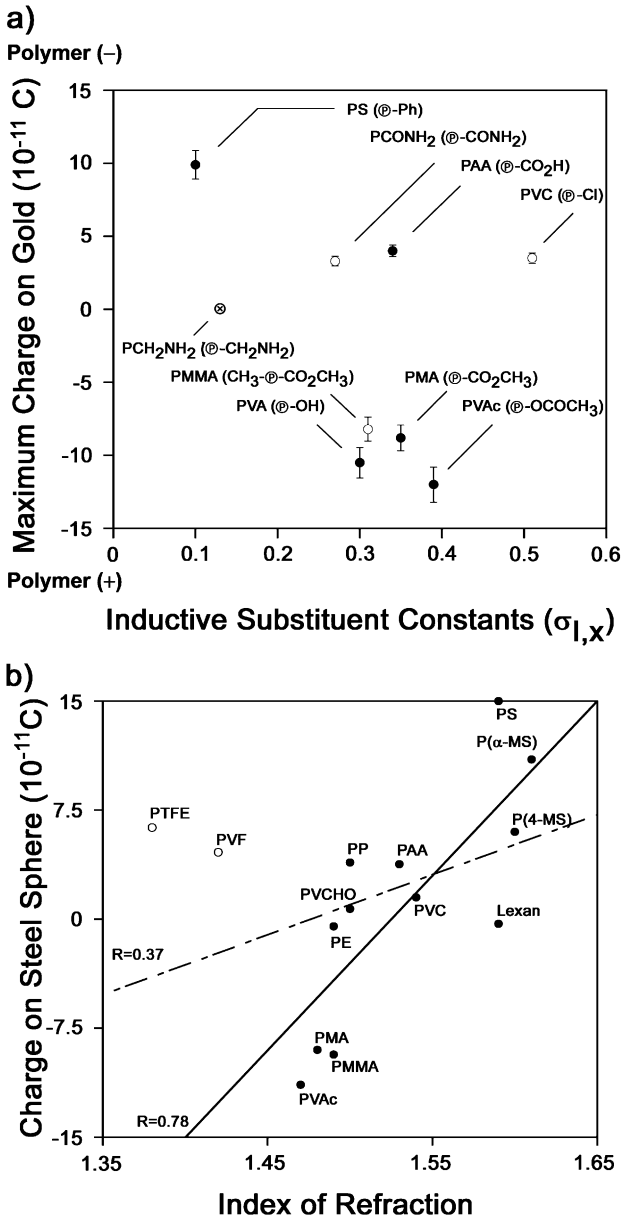


Figure 7. (a) Plot of the maximum charges measured on gold as a function of inductive substituent constants ($\sigma_{I,X}$, where X is the substituent on Ⓟ-X). Open markers (○) represent saturation data, and closed markers (●) represent the maximum magnitude of charges accumulated on a sphere before the sphere adhered to the film. The point for $PCH_2NH_2$ represented by ⊗ was measured at 6 °C; see Table 3. (b) Dependence of the charge developed on steel beads as a function of the index of refraction of the polymeric supports. The correlation coefficient for nonfluorinated polymers (closed markers) was 0.78; including fluorinated polymers (open markers) it was 0.37.

If an exclusive ion or proton transfer were responsible for charging, the p$K_a$ values for the functional groups of the polymers we studied might have correlated with the charges listed in Table 1. They did not. For example, PAA ($PCO_2H$) is much more acidic than $PCONH_2$, but both charge to similar magnitudes with the


(34) Veregin, R. P. N.; Tripp, C. P.; McDougall, M. N. V.; Osmond, D. *J. Imaging Sci. Technol.* **1995**, *39*, 429−432.
(35) Akande, A. R.; Lowell, J. *J. Phys. D: Appl. Phys.* **1987**, *20*, 565−578.
(36) Gibson, H. W.; Bailey, F. C. *Chem. Phys. Lett.* **1977**, *51*, 352−355.
(37) Gibson, H. W. *Can. J. Chem.* **1977**, *55*, 2637−2641.
(38) The ionization energy (the energy of the HOMO below vacuum) and the electron affinity (the energy of the LUMO below vacuum) both increase in proportion to $\sigma_{I,X}$ and are therefore proportional to one another.
(39) Akande, A. R.; Lowell, J. *J. Phys. D: Appl. Phys.* **1987**, *20*, 565−578.
(40) Shinohara, I.; Yamamoto, F.; Anzai, H.; Endo, S. *J. Electrost.* **1976**, *2*, 99−110.
(41) *CRC Handbook of Chemistry and Physics*, 81st ed.; Lide, D. R., Ed.; CRC Press: Boca Raton, FL, 2001; pp 12−124.

same polarities when spheres of metals and metal oxides roll on their surfaces. Furthermore, correlations of the measured charges in Table 1 should correlate with ionization potential and electron affinity of the polymers if an exclusive electron-transfer mechanism is operative. We were unable to make such a correlation.[40]

We briefly mention that the degree of charging did not correlate with the intrinsic properties of the polymers such as dielectric constant (correlation coefficient $R = 0.45$) or dielectric strength ($R = 0.28$). Interestingly, the developed charge showed significant correlation with the index of refraction of nonfluorinated polymers ($R = 0.78$; Figure 7b)—we were not able to rationalize this correlation, and we do not know whether it is simply fortuitous or whether it has a physical interpretation. In any event, we believe that contact charging on polymers will prove to be a multifactorial phenomenon and that it will take extensive study—certainly more extensive than can be included in this paper—to identify and characterize these factors.

## CONCLUSION

We described a sensitive tool—built from readily available components—for studying contact electrification of metals and metal oxides on polymeric insulators. Unlike previous measuring devices, this analytical system measures charge noninvasively using a technique in which the metallic sphere is isolated from the electrode; this isolation prevents loss of charge from the sphere during measurement. Because the measurement of charge is noninvasive (that is, it does not require physical contact with the measuring electrode), we are able to monitor the charge as it accumulates on a sphere and measure the kinetics of charging. This system allows rapid survey of the ability of polymeric surfaces to charge by contact electrification and assessment of their kinetics of charging: we quantified the contact charging of spheres rolling on the surfaces of polymeric slabs and generated an internally consistent set of data that included the polarity and magnitude of charging for a homologous series of polymers. We believe our system has the simplicity required for it to serve broadly in programs of screening designed to suggest relations between molecular structure and macroscopic behavior in charging.

## EXPERIMENTAL SECTION

Stainless steel spheres (type 316, 1 mm in diameter) were purchased from Small Parts (Miami Lakes, FL). The spheres were washed successively with methylene chloride, hexanes, methanol, and acetone, were dried in an oven at 60 °C for 1 h, and were stored under an atmosphere of dry nitrogen gas until use. Spheres coated with gold and silver were prepared by thermally evaporating (Edwards Auto 306) an adhesion-promoting layer of chromium (30 nm at a rate of 0.2 nm/s), followed by evaporation of the desired metal (300 nm at a rate of 0.2 nm/s) onto stainless steel spheres. Mechanical agitation of the spheres during evaporation of metal ensured complete and even coverage of the metal on the surfaces of the spheres. The finished spheres were stored under an atmosphere of dry nitrogen gas until use to prevent unwanted oxidation or contamination of the surfaces. Spheres coated with a gold oxide layer were prepared just prior to use by oxidation of spheres coated with gold for1 h using UV light and ozone[42] (Boekel UV/ozone cleaner, model 135500). Spheres coated with an oxidized layer of silver were prepared by treatment of silver-coated stainless steel spheres with a 30% solution of hydrogen peroxide (5 min, until formation of gas ceased); the treated spheres were dried under a stream of nitrogen gas and further dried in an oven at 60 °C for 1 h.

Pyrex surfaces (Petri dishes) were rinsed with methylene chloride and ethanol and dried in an oven at 100 °C before use. Polystyrene surfaces (Petri dishes, VWR) were used as received. Solutions of polymers were obtained from Aldrich and Polysciences. Films of PE, PHMA, PMA, and PMMA were cast from solutions of toluene; films of PAA, $PCONH_2$, $PCH_2NH_2$, and PVA were cast from aqueous solutions; films of PVAc were cast from solutions of methylene chloride; films of Lexan, Mylar, Nylon, PVC, and Teflon were obtained from Small Parts and Comco-Graphics (Devens, MA). All cast films (~100 $\mu$m) were dried overnight at 60 °C, unless noted otherwise. Films of PAA were esterified by reaction (≤1 h) with the vapor of diethyl ether that contained diazomethane.[43]

The charge that accumulated on the spheres was measured using an electrometer (Keithley 6517) operating at the nanocoulomb scale. All data were collected at 21−24% RH and 23 °C, unless noted otherwise.

## ACKNOWLEDGMENT

This work was supported by the U.S. Department of Energy (Award 00ER45852). J.A.W. gratefully acknowledges support from the Natural Sciences and Engineering Research Council of Canada.

Received for review March 18, 2003. Accepted July 3, 2003.

AC034275J

(42) King, D. E. *J. Vac. Sci. Technol. A* **1995**, *13*, 1247−1253.
(43) Leonard, J.; Lygo, B.; Procter, G. *Advanced Practical Organic Chemistry*, 2nd ed.; Chapman & Hall: London, 1995; pp 103−106.